Physica E 43 (2011) 1050–1055

Contents lists available at ScienceDirect

Physica E

journal homepage: www.elsevier.com/locate/physe

Small scale effects on the stability of carbon nano-peapods under radial pressure

M. Asghari [a], R. Naghdabadi [a,b,*], J. Rafati-Heravi [a]

[a] Department of Mechanical Engineering, Sharif University of Technology, Tehran, Iran
[b] Institute for Nano Science and Technology, Sharif University of Technology, Tehran, Iran

ARTICLE INFO

Article history:
Received 26 July 2010
Received in revised form
10 November 2010
Accepted 17 December 2010
Available online 22 December 2010

ABSTRACT

In this paper, a nonlocal elasticity formulation is presented for analyzing the instability of nano-peapods by modeling the nanotube as a shell. Using the nonlocal elasticity theory, the small scale characteristics of Carbon Nano-Peapods (CNPs) are taken into account. While the classical elastic shell model overestimates the critical pressure for the onset of structural instability of carbon nanotubes, the obtained results show that the nonlocal elastic shell model for nano-peapods can potentially provide better predictions. According to the results, it is concluded that the presence of C_{60} inside (10,10) Carbon Nanotubes (CNTs) significantly increases the stability resistance of the single CNT.

1. Introduction

After discovery of Carbon Nanotubes (CNTs) by Iijima [1], it has been observed that CNTs can also encapsulate some types of nanostructures and construct a self-assembled hybrid structures. Atoms and molecules such as He, Xe, H_2, CO, CO_2 and CH_4 [2–4], bio-molecules like DNA [5] and "buckminsterfullerenes" or simply "fullerenes" like C_{60} molecules [6,7] may be absorbed inside CNTs. The hybrid structure of fullerenes inside a CNT is denoted by $C_k@(r,s)$ and called a Carbon Nano-Peapod (CNP) or C_k-peapod in short, where C_k symbolizes the nested fullerene with k atoms of carbon, and Hamada indices (r,s) specifies the chirality of the host CNT [8]. Unique physical and mechanical characteristics of nano-peapods apprised from experimental observations, directed researchers to look for various potential applications of these nano-structures [9,10]. Hence, it is useful to study the behavior of these nano-structures for possible future applications.

Nano-sized experiments are actually difficult and expensive. Also, atomic-based analyses like Molecular Dynamics (MD) are relatively time-consuming and expensive for large-sized systems [11]. Therefore, continuum based modeling can be utilized for analysis of nano-structures to arrive at some estimated results with much less computational efforts. Continuum based modeling has been employed by researchers specially to study the mechanical behavior of CNTs, i.e. to study the vibration analysis [12], wave propagation [13], axial buckling [14,15], torsional buckling [16], buckling under bending moment [17] and buckling under radial pressure [18]. In addition, continuum based modeling of nano-peapods has been employed by Sohi and Naghdabadi to study the stability of C_{60}-peapods under pressure [19], and combined axial compressive loading and external radial pressure [20] using the classical Donnell's shell model.

In nano-structures, the lattice spacing between individual atoms is considerable with respect to the structural dimensions, so that utilizing the classical continuum based methods with the assumption of the continuity of the structure for analyzing them is essentially doubtful [21–23]. Eringen [24,25] has substantiated the idea that small scale effects should be taken into account in the continuum theories for the study of structures with small size features and proposed a non-classical continuum theory named as the nonlocal theory. Peddieson et al. [23] were the first who insisted on the feasibility and applicability of the nonlocal continuum theory in the nanotechnology. In recent years, considerable attention has been turned to the application of the nonlocal elasticity theory for the analysis of the mechanical stability and vibration of single- and multi-walled carbon nanotubes [11,23,26–28].

Zhang et al. derived the elastic shell equations with importing the small scale effects into the classical shell equations, and employed this model to analyze the buckling of CNT under axial forces [29] and hydrostatic pressure [30]. Li and Kardomateas [21] studied thermal buckling of CNT using the nonlocal elastic shell model.

In this paper, utilizing the nonlocal theory for taking into account the small scale effects, the stability of $C_{60}@(10,10)$ CNP under radial pressure is investigated by modeling the host CNT as the Donnel's nonlocal elastic shell model.

* Corresponding author at: Department of Mechanical Engineering, Sharif University of Technology, Tehran, Iran. Tel.: +98 21 66165546; fax: +98 21 66000021.
E-mail addresses: asghari@sharif.edu (M. Asghari), naghdabd@sharif.edu (R. Naghdabadi).

1386-9477/$ - see front matter © 2011 Published by Elsevier B.V.
doi:10.1016/j.physe.2010.12.013

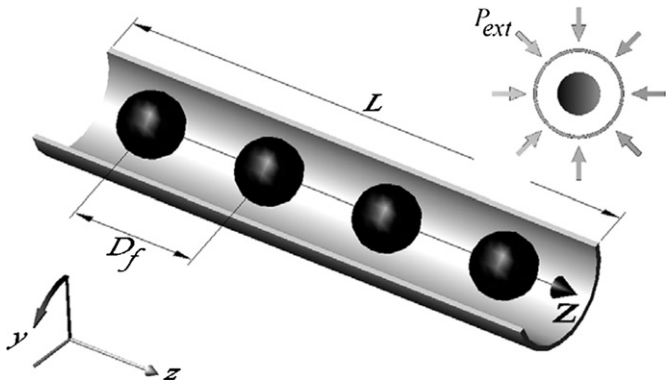

Fig. 1. C_{60} at SWCNT nano-peapod under external pressure p_{ext} [19].

2. Interaction between the host CNT and the nested fullerenes

The non-bonded Van der Waals (vdW) interactions between the nested fullerenes and the host carbon nanotube (Fig. 1) can be described using Lenard–Jones potential as

$$\phi_{ij} = \frac{A}{\mu^6}\left[\frac{1}{2}y_0^6\left(\frac{\mu}{r_{ij}}\right)^{12} - \left(\frac{\mu}{r_{ij}}\right)^{6}\right], \tag{1}$$

where $A=24.3\times10^{-79}$ J m^6, $\mu=1.42$ Å, $y_0=2.7$ [31], and r_{ij} denotes the distance between atom i of the innermost CNT layer and atom j of C_{60}. The total vdW inter-atomic potential energy of nano-peapod is obtained using Eq. (1) by summing up i and j, for taking into account the effects of interaction between all atoms of the fullerene and those of the innermost nanotube. The C_{60} molecules, in the case of high density packing, portray a linear one-dimensional crystal into (10,10) CNT with lattice equilibrium distance $D_f\approx1$ nm [6,7,32,33].

In view of the ordered arrangement of the nested C_{60} fullerenes inside the host CNT, the internal radial pressure enforced by C_{60} on the host CNT wall $p_{vdW,C_{60}}$ is considered to have approximately a harmonic distribution as the following expression:

$$p_{vdW,C_{60}}(z) = a_0 + \sum_n\left[a_n\cos\left(\frac{2n\pi z}{D_f}\right) + b_n\sin\left(\frac{2n\pi z}{D_f}\right)\right], \tag{2}$$

where a_n and b_n are the Fourier series multipliers. It is recalled that the parameter D_f is the lattice equilibrium distance between fullerenes. In this paper, the *vdW* internal pressure distribution exerted by C_{60} encapsulated fullerenes on (10,10) CNT is considered in accordance with what reported in Ref. [19].

3. Nonlocal elastic shell equations

3.1. A brief review on the nonlocal elasticity theory

In the classical theory of elasticity, the stress tensor $\boldsymbol{\sigma}$ at the reference point $\mathbf{x}$ of a continuous body is a function of only the local point strain tensor $\boldsymbol{\varepsilon}$ at $\mathbf{x}$. Eringen [24] proposed the idea that for taking into account the small scale effects, the constitutive equations should be modified. Towards this end, he presented the nonlocal elasticity theory, in which the constitutive equations relate the stress tensor $\boldsymbol{\sigma}$ at the local point $\mathbf{x}$ to strain tensor $\boldsymbol{\varepsilon}$ at all points of a continuous body Ω, both local and nonlocal points. The constitutive equation in the nonlocal elasticity theory is displayed in the integral form as [25]

$$\sigma(\mathbf{x}) = \iiint_{\Omega}\psi(|\mathbf{x}'-\mathbf{x}|,\tau)\quad \mathbf{C}:\boldsymbol{\varepsilon}(\mathbf{x}')dV(\mathbf{x}'), \tag{3}$$

where function $\psi(|\mathbf{x}'-\mathbf{x}|,\tau)$ is called the nonlocal modulus, $|\mathbf{x}'-\mathbf{x}|$ is the distance between a local point $\mathbf{x}$ and a nonlocal point $\mathbf{x}'$, $\mathbf{C}$ denotes the fourth order elasticity tensor, and $\tau=e_0a/l$, with a as the internal characteristic length (e.g. C–C bond length or granular size), l as the external characteristic length (e.g. crack length or wave length) and e_0 as a material parameter determined for a nano-structure to coincide its experimental and continuum model results [11,21,25]. Based on the integral form presented in Eq. (3), Eringen developed the differential form of constitutive equation of the nonlocal elasticity theory as follows [11,21,25,30]

$$(1-\eta^2\nabla^2)\boldsymbol{\sigma} = \mathbf{C}:\boldsymbol{\varepsilon}, \tag{4}$$

with $\eta=e_0a$ is the small scale coefficient. Eq. (4) can be written in the component form as

$$(1-\eta^2\nabla^2)\sigma_{ij} = \mathbf{C}_{ijkl}\boldsymbol{\varepsilon}_{kl}. \tag{5}$$

It is noted that, in the special case of $\eta=e_0a\to0$, i.e. when the internal characteristic length is negligible with respect to the external characteristic length, the nonlocal elasticity constitutive equation (Eq. (5)) approaches the classical elasticity constitutive equation $\sigma_{ij}=\mathbf{C}_{ijkl}\boldsymbol{\varepsilon}_{kl}$.

3.2. A nonlocal elastic shell model for carbon nanotubes

Consider a cylindrical shell with a length L and thickness h for modeling the nanotube (see Fig. 1). Let x, y and z be the radial, circumferential and axial coordinates of a nanotube, respectively, and also u, v and w the corresponding mid-surface displacement components. Considering Donnell's assumptions for shells, the following relations between components of the strain tensor and the displacement vector can be written [21,30]

$$\varepsilon_z = \varepsilon_{0z} - xw_{,zz},\quad \varepsilon_y = \varepsilon_{0y} - xw_{,yy},\quad \gamma_{zy} = \gamma_{0zy} - xw_{,zy}, \tag{6}$$

where ε_{0z}, ε_{0y} and γ_{0zy} are strain components of the middle surface of the shell that can be demonstrated as

$$\varepsilon_{0z} = u_{,z},\quad \varepsilon_{0y} = v_{,y} + \frac{w}{R},\quad \gamma_{0xy} = u_{,y} + v_{,z}, \tag{7}$$

where R is the radius of the mid-surface of the nanotube and comma denotes differentiation with respect to the following index [18,21]. Considering axisymmetric conditions, the nonlocal elasticity constitutive equations can be represented as [21,30]

$$\begin{aligned}
(1-\eta^2\nabla^2)\sigma_z &= \frac{E}{1-\upsilon^2}(\varepsilon_z + \upsilon\varepsilon_y)\\
(1-\eta^2\nabla^2)\sigma_y &= \frac{E}{1-\upsilon^2}(\varepsilon_y + \upsilon\varepsilon_z)\\
(1-\eta^2\nabla^2)\sigma_{zy} &= \frac{E}{2(1+\upsilon)}\gamma_{zy},
\end{aligned} \tag{8}$$

where $\nabla^2=\partial^2/\partial z^2+\partial^2/\partial y^2$ represents Laplacian operator, E is the elastic modulus, and υ is the Poisson's ratio.

The resultant forces and moments are related to the stress components as [21]

$$N_z = \int_{-h/2}^{h/2}\sigma_z\,dx,\quad N_y = \int_{-h/2}^{h/2}\sigma_y\,dx,\quad N_{zy} = \int_{-h/2}^{h/2}\sigma_{zy}\,dx, \tag{9}$$

$$M_z = \int_{-h/2}^{h/2}\sigma_z r\,dr,\quad M_y = \int_{-h/2}^{h/2}\sigma_y r\,dr,\quad M_{zy} = \int_{-h/2}^{h/2}\sigma_{zy} r\,dr. \tag{10}$$

By substituting Eqs. (6) and (7) into Eq. (8), and then combining the results by Eqs.(9) and (10), one can get the following expressions for the resultant forces and moments

$$\begin{aligned}
(1-\eta^2\nabla^2)N_z &= K(u_{,z} + \upsilon v_{,y} + \upsilon w/R)\\
(1-\eta^2\nabla^2)N_y &= K(v_{,y} + \upsilon u_{,z} + w/R)\\
(1-\eta^2\nabla^2)N_{zy} &= \frac{1-\upsilon}{2}K(u_{,y} + v_{,z})\\
(1-\eta^2\nabla^2)M_z &= -D(w_{,zz} + \upsilon w_{,yy})
\end{aligned}$$

$$(1-\eta^2\nabla^2)M_y = -D(w_{,yy}+\upsilon w_{,zz})$$
$$(1-\eta^2\nabla^2)M_{zy} = -D(1-\upsilon)w_{,zy}, \tag{11}$$

where $D=Eh^3/12(1-\upsilon^2)$ stands for the effective bending stiffness of the shell [21,30], and $K=Eh/(1-\upsilon^2)$. On the other hand, the equilibrium equations for the shell can be written as

$$(1-\eta^2\nabla^2)N_{z,z}+(1-\eta^2\nabla^2)N_{zy,y}=0 \tag{12}$$

$$(1-\eta^2\nabla^2)N_{yz,x}+(1-\eta^2\nabla^2)N_{y,y}=0 \tag{13}$$

$$(1-\eta^2\nabla^2)M_{z,zz}+2(1-\eta^2\nabla^2)M_{zy,zy}+(1-\eta^2\nabla^2)M_{y,yy} -(1-\eta^2\nabla^2)\Im(w)-(1-\eta^2\nabla^2)\frac{1}{R}N_y+(1-\eta^2\nabla^2)p(z,y)=0, \tag{14}$$

where $\Im$ is a differential operator defined as

$$\Im = N_z\frac{\partial^2}{\partial z^2}+2N_{zy}\frac{\partial^2}{\partial z\partial y}+N_y\frac{\partial^2}{\partial y^2}. \tag{15}$$

Substituting the resultants forces and moments from Eq. (11) into the equilibrium Eqs. (12)–(14), then eliminating axial and circumferential displacement components, the nonlocal Donnell's equilibrium equation for a nanotube is obtained as [21]

$$D\nabla^8 w+\frac{Eh}{R^2}\frac{\partial^4 w}{\partial z^4}-(1-\eta^2\nabla^2)\nabla^4\Im(w)=(1-\eta^2\nabla^2)\nabla^4 p(z,y). \tag{16}$$

With $\eta=e_0a\to 0$, i.e. ignoring the small scale effects, Eq. (16) approaches the well-known classical Donnell's shell stability equation.

4. Instability of carbon nano-peapods under radial pressure

In case of a single-walled carbon nano-peapod under external radial pressure p_{ext}, the axial stress and also shearing stresses vanish. Also, the circumferential stress is due to only possible *vdW* pressure exerted on the CNT wall. Hence, the following expressions can be written for the axial, shearing and circumferential resultants

$$N_z=N_{zy}=0, \quad N_y=R[-p_{ext}+p_{vdw,C60}(z)], \tag{17}$$

By substitution of Eq. (17) into Eq.(15), the operator $\Im$ can be obtained as

$$\Im = R\left[-p_{ext}+p_{vdw,C60}(z)\right]\frac{\partial^2}{\partial y^2}, \tag{18}$$

Now, inserting operator $\Im$ from Eq. (18) into the differential equation governing the radial deformation of the CNT (Donnell's nonlocal elastic shell Eq. (16)), one can arrive at the equilibrium equation of CNP as follows:

$$D\nabla^8 w+\frac{Eh}{R^2}\frac{\partial^4 w}{\partial z^4}-(1-\eta^2\nabla^2)\nabla^4\left\{R\left[-p_{ext}+p_{vdW,C60}(z)\right]\frac{\partial^2}{\partial y^2}\right\}w -(1-\eta^2\nabla^2)\nabla^4[-p_{ext}+p_{vdW,C_{60}}(z)]=0, \tag{19}$$

At any equilibrium condition with the infinitesimal deformation relative to the initial unloaded state for the nano-peapods under radial external pressure, Eq. (19) should be satisfied. In stable equilibrium conditions of any structure, if the observed deformed state is perturbed with another deformation, this added deformation will automatically be damped and the structure keeps the previous shape in the equilibrium state. On the other hand, in unstable equilibrium conditions, the imposed perturbed deformation will grow and the structure will not return to the initial deformed equilibrium condition. If the loading is exactly equal to the critical value, neither lower to cause the perturbations to be damped nor greater to cause them to grow, the perturbed deformed configuration is also in equilibrium. Let function w describe the deformation of CNT of the nano-peapod in equilibrium conditions under the critical radial pressure p_{cr}, and function $\tilde{w}$ represent the special perturbation which will grow and cause the instability of the nano-peapod when the external radial pressure becomes even slightly more than p_{cr}. Hence, Eq. (19) will also be valid if w are replaced with $w+\tilde{w}$. By subtracting the new equations from Eq. (19), the following equations can be obtained in terms of the perturbation function $\tilde{w}$:

$$D\nabla^8\tilde{w}+\frac{Eh}{R^2}\frac{\partial^4\tilde{w}}{\partial z^4}-(1-\eta^2\nabla^2)\nabla^4\left\{R\left[-p_{ext}+p_{vdW,C_{60}}(z)\right]\frac{\partial^2}{\partial y^2}\right\}\tilde{w}=0. \tag{20}$$

A trial perturbation function for $\tilde{w}$ can be assumed as sinusoidal harmonics with m axial lobes (azimuthal) and n circumferential half-waves as

$$\tilde{w}=\tilde{W}\sin(\alpha z)\sin(\beta y), \tag{21}$$

where

$$\alpha=\frac{m\pi}{L}, \quad \beta=\frac{n}{R}, \tag{22}$$

and $\tilde{W}$ is the amplitude of the radial deflection caused by the perturbation on the CNT layer, with m and n as arbitrary positive integers. Substituting the proposed radial deflection function (21) into Eq. (20), the following algebraic linear equation is obtained:

$$\tilde{A}\sin(\alpha z-\beta y)=0, \tag{23}$$

where

$$\tilde{A}=D(\alpha^2+\beta^2)^4\,\tilde{W}+\frac{Eh}{R^2}\alpha^4\,\tilde{W}+R\beta^2\left(\frac{d^4}{dz^4}-\eta^2\frac{d^6}{dz^6}\right)p_{vdw,C_{60}}(z)\tilde{W} +[1+\eta^2(\alpha^2+\beta^2)](\alpha^2+\beta^2)^2\left\{R\beta^2\left[-p_{ext}+p_{vdW,C_{60}}(z)\right]\right\}\tilde{W}=0. \tag{24}$$

To satisfy Eq. (24) at all z and y, the coefficient $\tilde{A}$ should vanish. Consequently, we have $\overline{A}(\alpha,\beta)=\int_0^L\tilde{A}(\alpha,\beta,z)\,dz=0$, which results in

$$\left\{D(\alpha^2+\beta^2)^4+\frac{Eh}{R^2}\alpha^4+\frac{R}{L}\beta^2\left(\frac{d^3p_{vdw,C_{60}}(z)}{dz^3}-\eta^2\frac{d^5p_{vdw,C_{60}}(z)}{dz^5}\right)\Big|_0^L +R\left[1+\eta^2(\alpha^2+\beta^2)\right](\alpha^2+\beta^2)^2\beta^2\left(-p_{ext}+\frac{1}{L}\int_0^L p_{vdw,C_{60}}(z)dz\right)\right\}\tilde{W}=0. \tag{25}$$

Using Eq. (25), the critical radial pressure at the onset of structural instability of the carbon nano-peapod can be numerically obtained. For specific values m and n, recalling $\alpha=m\pi/L$, $\beta=n/R$, the radial pressure corresponding to (m,n) mode of perturbation can be achieved with the aid of Eq. (25) as follows:

$$p_{ext}\big|_{m,n}=\frac{1}{L}\int_0^L p_{vdw,C_{60}}(z)dz +\frac{\left\{D(\alpha^2+\beta^2)^4+\frac{Eh}{R^2}\alpha^4\right\}+\frac{R}{L}\beta^2\left(\frac{d^3p_{vdw,C_{60}}(z)}{dz^3}-\eta^2\frac{d^5p_{vdw,C_{60}}(z)}{dz^5}\right)\Big|_0^L}{R[1+\eta^2(\alpha^2+\beta^2)](\alpha^2+\beta^2)^2\beta^2}. \tag{26}$$

The critical radial pressure p_{cr} of the carbon nano-peapod can be determined by finding the minimum values of $p_{ext}|_{m,n}$ in Eq. (26) for different m and n.

5. Numerical results and discussion

In this section, some numerical examples are provided by utilizing the derived Eq. (26) to obtain the critical radial pressure

of C_{60}@(10,10) CNP based on the nonlocal elastic shell, noting that C_{60}@(10,10) CNP is a specific case of nano-peapods that many studies have been published which investigate its properties [34–38]. The values used for some parameters in the numerical investigations are considered to be $D=0.85$ eV $Eh=360$ J m^{-2}, $h=0.34$ nm and $R=0.678$ nm [17,39]. First, we consider a single (10,10) CNT with $L=9.5$ nm. The calculated critical radial pressure p_{cr} for different values of the small scale coefficient $\eta=e_0a$ has been depicted in Fig. 2, for a common range of η, i.e. the range below 1 nm for carbon nanotubes [21,40]. It is noted that all the numerical results have been obtained by using one term approximation in the summation presented by Eq. (2).

The critical pressure is obtained equal to 1.7 GPa based on the classical continuum model, i.e. the result corresponding to $\eta=0$ nm, while the result reported from Molecular Dynamics (MD) simulation is 1.55 GPa [41]. It can be seen from Fig. 2 that the nonlocal model employed in this paper gives a lower value for the critical pressure with respect to the classical model. This lower estimation causes diminishing of the deviation of classical continuum based result from the MD simulations. The first buckling mode is observed at $(m,n)=(1,1)$ which means that the tube cross section transforms into an elliptical shape, noting this is a common agreement between our prediction and MD [41]. From Fig. 2, it is observed that with a value between 0.1 and 0.2 nm for the scale coefficient $\eta=e_0a$, the nonlocal model predicts the critical pressure in a good agreement with respect to the MD simulation.

Now, the effect of filling the (10,10) nanotube by a high density packing of C_{60} fullerenes with approximately $D_f=1$ nm [7,32,33] is investigated. In Fig. 3, the obtained results for the critical pressure versus the scale coefficient $\eta=e_0a$ for C_{60} at (10,10) nano-peapod is presented.

As observed in Fig. 3, the presence of the encapsulated C_{60} fullerenes inside the (10,10) CNT causes an increase in the critical radial pressure. This means that the (10,10) CNT with C_{60} fullerenes is more stiffer and the resistance against the instability is more. In Fig. 4, the increased percentage in the critical radial pressure of (10,10) CNT due to the presence of encapsulated C_{60} fullerenes is plotted versus scale coefficient $\eta=e_0a$.

The prediction of this work for the increase in the stability resistance of (10,10) CNT due to the presence of C_{60} fullerenes has also been reported before for different types of loading including axial compressive force [35,42], the bending moment [37] and the torsional moment [36,38] using MD simulations.

6. Conclusions

The continuum based methods are utilized in the prediction of the mechanical behavior of nano-structures because of difficulties in applying other approaches such as Molecular Dynamics (MD) simulations for their high computational costs. However, the classical continuum theory is not capable to suitably treat the nano-structures with discontinuities. The nonlocal continuum theory, as a non-classic continuum theory, includes the parameters which can reflect the size-dependent behavior of nano-structures and can be implemented more reasonably for analyzing the mechanical behavior of nano-structures with retaining the benefits of continuum based approaches. In this work, a formulation has been introduced for investigating the instability of carbon nano-peapods under radial external pressure based on the nonlocal elasticity theory by modeling the nanotube as the Donnell shell. The comparison between numerical results obtained in the case studies for the buckling pressure of the C_{60} at (10,10) nano-peapod with those corresponding to the (10,10) single nanotube demonstrate that the stability resistance increases more than 100% due to the presence of C_{60} in the nanotube. This outcome on the increase of the stability resistance due to the presence of C_{60} is in good agreement with some MD simulations studying the instability of C_{60} at (10,10) nano-peapod under torsional moment [36,38].

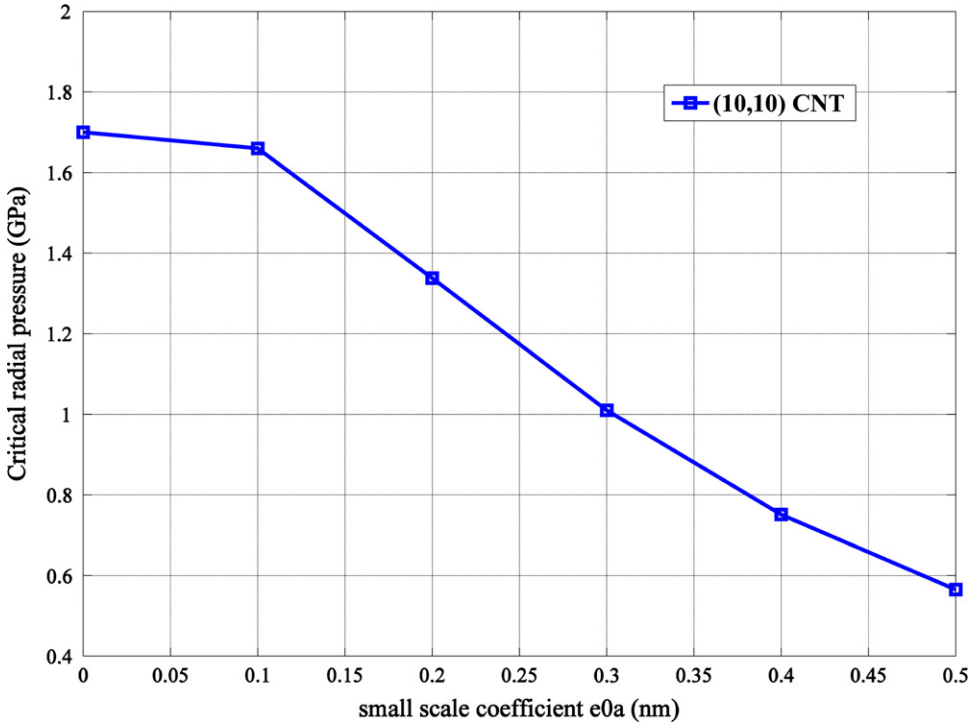

Fig. 2. Critical radial pressure of (10,10) CNT versus scale coefficient $\eta=e_0a$.

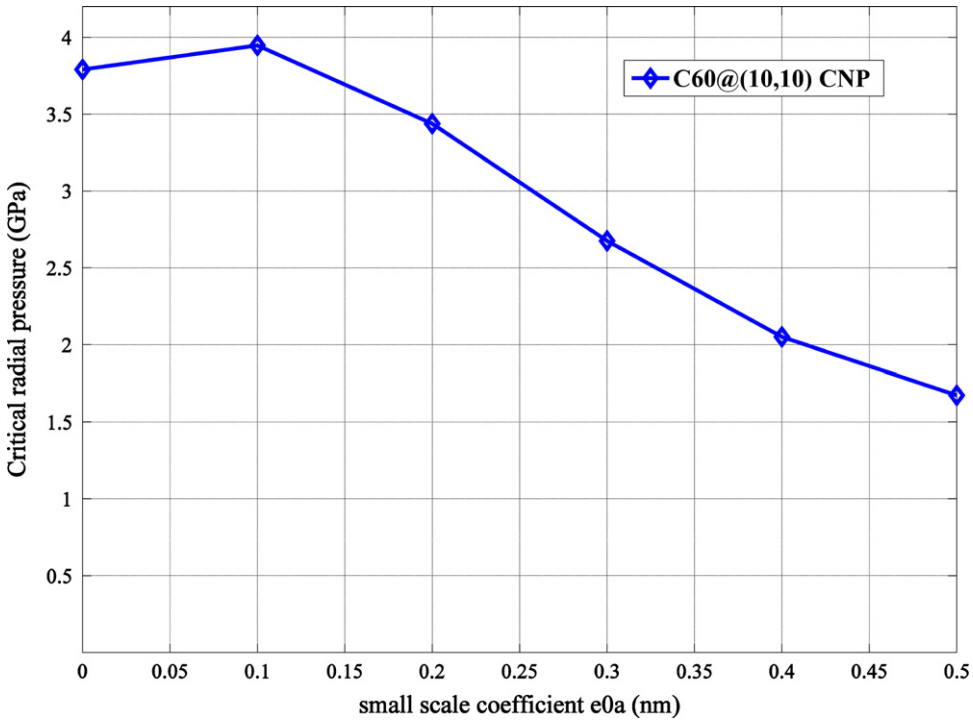

Fig. 3. Critical radial pressure of C_{60}@(10,10) CNP versus the scale coefficient $\eta = e_0 a$.

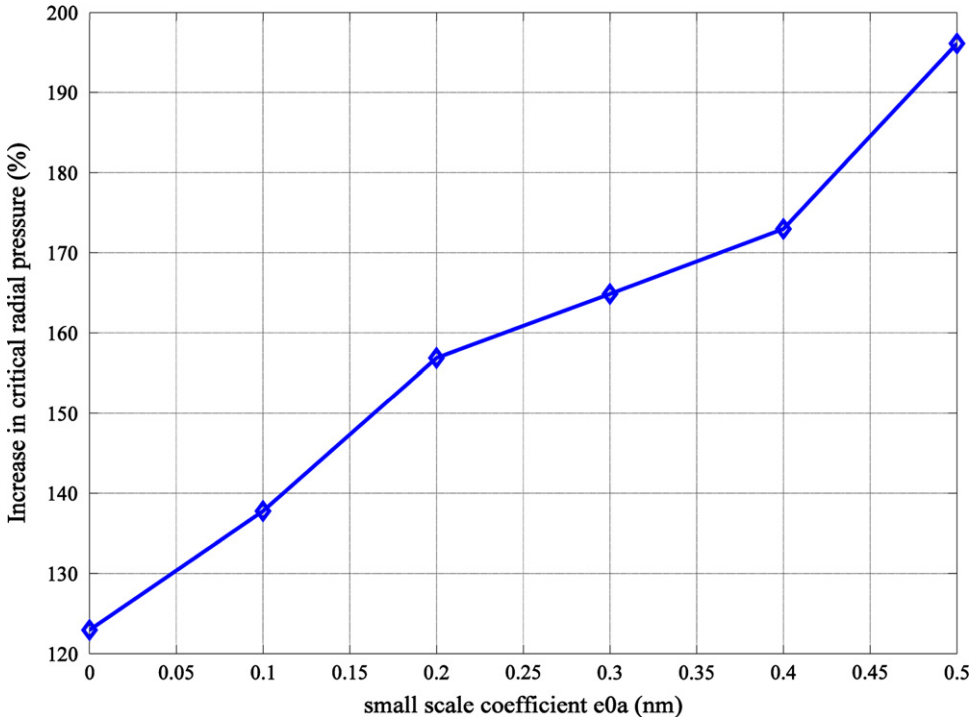

Fig. 4. Increased percentage of the critical radial pressure of (10,10) CNT due to the presence of encapsulated C_{60} fullerenes versus scale coefficient $\eta = e_0 a$.

References

[1] S. Iijima, Nature 354 (1991) 56.
[2] M.S. Dresselhaus, K.A. Williams, P.C. Eklund, MRS Bull. 24 (1999) 45.
[3] A. Kuznetsova, D.B. Mawhinney, V. Naumenko, J.T. Yates Jr, J. Liu, R.E. Smalley, Chem. Phys. Lett. 321 (2000) 292.
[4] M.W. Cole, V.H. Crespi, G. Stan, C. Ebner, J.M. Hartman, S. Moroni, M. Boninsegni, Phys. Rev. Lett. 84 (2000) 3883.
[5] H. Gao, Y. Kong, D. Cui, C.S. Ozkan, Nano Letter 3 (2003) 471.
[6] B.W. Smith, M. Monthioux, D.E. Luzzi, Chem. Phys. Lett. 315 (1999) 31.
[7] B.W. Smith, M. Monthioux, D.E. Luzzi, Nature 396 (1998) 323.
[8] N. Hamada, S.-i. Sawada, A. Oshiyama, Phys. Rev. Lett. 68 (1992) 1579.
[9] J.W. Kang, H.J. Hwang, Mater. Sci. Eng. C 25 (2005) 843.
[10] R.F. Service, Science 292 (2001) 345.
[11] T. Murmu, S.C. Pradhan, Physica E 41 (2009) 1232.
[12] J. Yoon, C. Ru, A. Mioduchowski, Compos. Sci. Technol. 63 (2003) 1533.
[13] L. Wang, H. Hu, Phys. Rev. B 71 (2005) 195412.
[14] C.Q. Ru, J. Appl. Phys. 89 (2000) 3425.
[15] A.R. Ranjbartoreh, A. Ghorbanpour, B. Soltani, Physica E 39 (2007) 230.

[16] Q. Wang, S.T. Quek, V.K. Varadan, Phys. Lett. A 367 (2007) 135.
[17] H.K. Yang, X. Wang, Model. Simulation Mater. Sci. Eng. 14 (2006) 99.
[18] C.Q. Ru, Phys. Rev. B: Condens. Matter 62 (2000) 10405.
[19] A.N. Sohi, R. Naghdabadi, Acta. Mater. 55 (2007) 5483.
[20] A.N. Sohi, R. Naghdabadi, Physica E 41 (2009) 513.
[21] R. Li, G.A. Kardomateas, ASME J. Appl. Mech. 74 (2007) 399.
[22] R. Li, G.A. Kardomateas, J. Appl. Mech.-T. ASME 74 (2007) 1087.
[23] J. Peddieson, G.R. Buchanan, R.P. McNitt, Int. J. Eng. Sci. 41 (2003) 305.
[24] A.C. Eringen, Int. J. Eng. Sci. 10 (1972) 1.
[25] A.C. Eringen, J. Appl. Phys. 54 (1983) 4703.
[26] M. Aydogdu, Physica E 41 (2009) 1651.
[27] J.N. Reddy, Int. J. Eng. Sci. 45 (2007) 288.
[28] J. Yang, L.L. Ke, S. Kitipornchai, Physica E 42 (2010) 1727.
[29] Y.Q. Zhang, G.R. Liu, X. Han, Phys. Rev. B 70 (2004) 1.
[30] Y.Q. Zhang, G.R. Liu, X. Han, Phys. Lett. A 349 (2006) 370.
[31] D. Qian, W.K. Liu, R.S. Ruoff, J. Phys. Chem. B 105 (2001) 10753.
[32] K.S. Troche, V.R. Coluci, S.F. Braga, D.D. Chinellato, F. Sato, S.B. Legoas, Nano Letters 5 (2005) 349.
[33] M. Melle-Franco, H. Kuzmany, F. Zerbetto, J. Chem. B 107 (2003) 6986.
[34] S. Osaka, S. Saito, A. Oshiyama, Phys. Rev. Lett. 86 (2001) 3835.
[35] B. Ni, S. Sinnott, P. Mikulski, J. Harrisson, Phys. Rev. Lett. 88 (2002) 205505.
[36] Q. Wang, Carbon 47 (2009) 507.
[37] J. Zhu, Z.Y. Pan, Y.X. Wang, L. Zhou, Q. Jiang, Nanotechnology 18 (2007) 275702.
[38] B.-W. Jeong, J.-K. Lim, S.B. Sinnott, J. Appl. Phys. 101 (2007) 084309.
[39] X. Wang, H.K. Yang, K. Dong, Mater. Sci. Eng. A 404 (2005) 314.
[40] Y.-G. Hu, K.M. Liew, Q. Wang, X.Q. He, B.I. Yakobson, J. Mech. Phys. Solids 56 (2008) 3475.
[41] J. Zang, O. Aldás-Palacios, F. Liu, Commun. Comput. Phys. 2 (2007) 451.
[42] L. Zhou, B.E. Zhu, Z.Y. Pan, Y.X. Wang, J. Zhu, Nanotechnology 18 (2007) 275709.